Environ. Sci. Technol. **2010,** *44,* 5964–5970

Mechanistic Toxicity Assessment of Nanomaterials by Whole-Cell-Array Stress Genes Expression Analysis

NA GOU, ANNALISA ONNIS-HAYDEN, AND APRIL Z. GU*

Department of Civil & Environmental Engineering, 360 Huntington Avenue, Northeastern University, Boston, Massachusetts 02115

Received March 2, 2010. Revised manuscript received May 19, 2010. Accepted May 25, 2010.

This study performed mechanistic toxicity assessment of nanosilver (nAg) and nanotitanium dioxide anatase ($nTiO_2$_a) via toxicogenomic approach, employing a whole-cell-array library consisting of 91 recombinated *Escherichia coli K12* strains with transcriptional GFP-fusions covering most known stress response genes. The results, for the first time, revealed more detailed transcriptional information on the toxic mechanism of nAg and $nTiO_2$_a, and led to a better understanding of the mode of action (MOA) of metal and metal oxide nanomaterials (NMs). The detailed pathways network established for the oxidative stress system and for the SOS (DNA damage) repair system based on the temporal gene expression profiling data revealed the relationships and sequences of key genes involved in these toxin response systems. Both NMs were found to cause oxidative stress as well as cell membrane and transportation damage. Genotoxicity and DNA damage were also observed, although $nTiO_2$_a induced SOS response via previously identified pathway and nAg seemed to induce DNA repair via a pathway different from SOS. We observed that the NMs at lower concentration tend to induce more chemical-specific toxicity response, while at higher concentrations, more general global stress response dominates. The information-rich real-time gene expression data allowed for identification of potential biomarkers that can be employed for specific toxin detection and biosensor developments. The concentration-dependent gene expression response led to the determination of the No Observed Transcriptional Effect Level (NOTEL) values, which can be potentially applied in the regulatory and risk assessment framework as an alternative toxicity assessment end point.

Introduction

The growing production and use of engineered nanomaterials (NMs) makes it inevitable for them to release to the natural environment. However, the toxicity mechanism of these NMs is largely unknown even though there is sound evidence of their toxicity (*1, 2*). The currently available water toxicity assessment methods, such as WET (Whole Effluent Toxicity) and TIE (Toxicity Identification Evaluation) can provide useful ecotoxicological information for toxicants in aquatic system. However, they have certain limitations, such as being labor-intensive and time-consuming, which make them neither feasible nor sufficient for screening a large and ever-increasing number of emerging contaminants in our water and for providing timely information needed for regulatory decision making in order to eliminate or reduce the potential risks associated with these pollutants.

Toxicogenomics, in which transcription and expression levels of thousands of genes in an organism in response to environmental toxin are monitored (*3, 4*), promises a revolutionary new ground for monitoring and identifying the chemicals responsible for toxicity (*5, 6*), revealing the toxic mechanism and obtaining pollutant-specific molecular fingerprints (or biomarkers) for compound classification and identification (*7, 8*), The No Observed Transcriptional Effect Level (NOTEL), a new concept generated with the development of toxicogenomics, can potentially serve as a more informative and sensitive end point for screening effluents and unknown chemicals for toxicity and be incorporated into ecological risk assessment and regulatory framework (*4, 6, 9*). A number of recent studies have demonstrated the application of toxicogenomics technology (e.g., microarray-based methods) for environmental monitoring (*10, 11*). However, several limitations of the current microarray-based gene-profiling technology, such as a high-cost, complex procedure and condition-sensitive results, prohibit its further development and wide application in environmental monitoring.

We recently applied prokaryotic real-time gene expression profiling by using a comprehensive cell array consisting of transcriptional green fluorescent protein (GFP)-fused recombinant *Escherichia coli* strains for toxicity evaluation (*12*). Our proposed method, comparing to the microarray approach, requires simpler, faster, and more reliable assay procedures, has higher reusability, and provides the desirable flexibility for customization of the cell array. The substantial information available on the functions of the genes of *E. coli* allows for understanding, mapping, and visualizing systematic cellular response pathways and molecular events occurring as a response to chemical exposure. The library we used is measuring the genomic promoter activities, namely the transcription initiation, which we interpreted as the indicator of gene expression activity as employed by previous researchers (*13, 14*).

In this study, we conducted mechanistic toxicity assessment of nanosilver (nAg) and nanotitanium dioxide anatase ($nTiO_2$_a) using the prokaryotic real-time gene expression profiling method developed. The two NMs were chosen because they have wide commercialization application in various fields and therefore are likely to be present in the environment. Compound-specific and concentration-sensitive two-dimensional (genes and time) gene expression profiling for nAg and $nTiO_2$_a at various concentrations were obtained. The gene expression alterations as the result of exposure to these two NMs provided insights into the underlying toxic mechanisms of these two NMs. The NOTEL for both NMs is determined based on the dose−response curve, and potentially biomarkers have been identified.

Materials and Methods

Nanomaterials. nAg (~60 nm, NanoDynamics Inc., Buffalo, NY) and $nTiO_2$_a (10 nm, NanoStructured & Amorphous Materials, Houston, Texas) were prepared in M9 medium for a stock concentration of 1000 mg/L, which contains 1% of crude Bovine Serum Albumin (BSA) as dispersant. The stock solutions were sonicated in a High energy Cup-sonicator, ~90 Watt power for at least 15 min to maintain a better dispersion before the toxicity assays. Detailed characterization parameters for the same nanomaterials used in this study can be found in Bello et al. (*15*).

* Corresponding author e-mail: april@coe.neu.edu.

10.1021/es100679f
Published on Web 06/29/2010

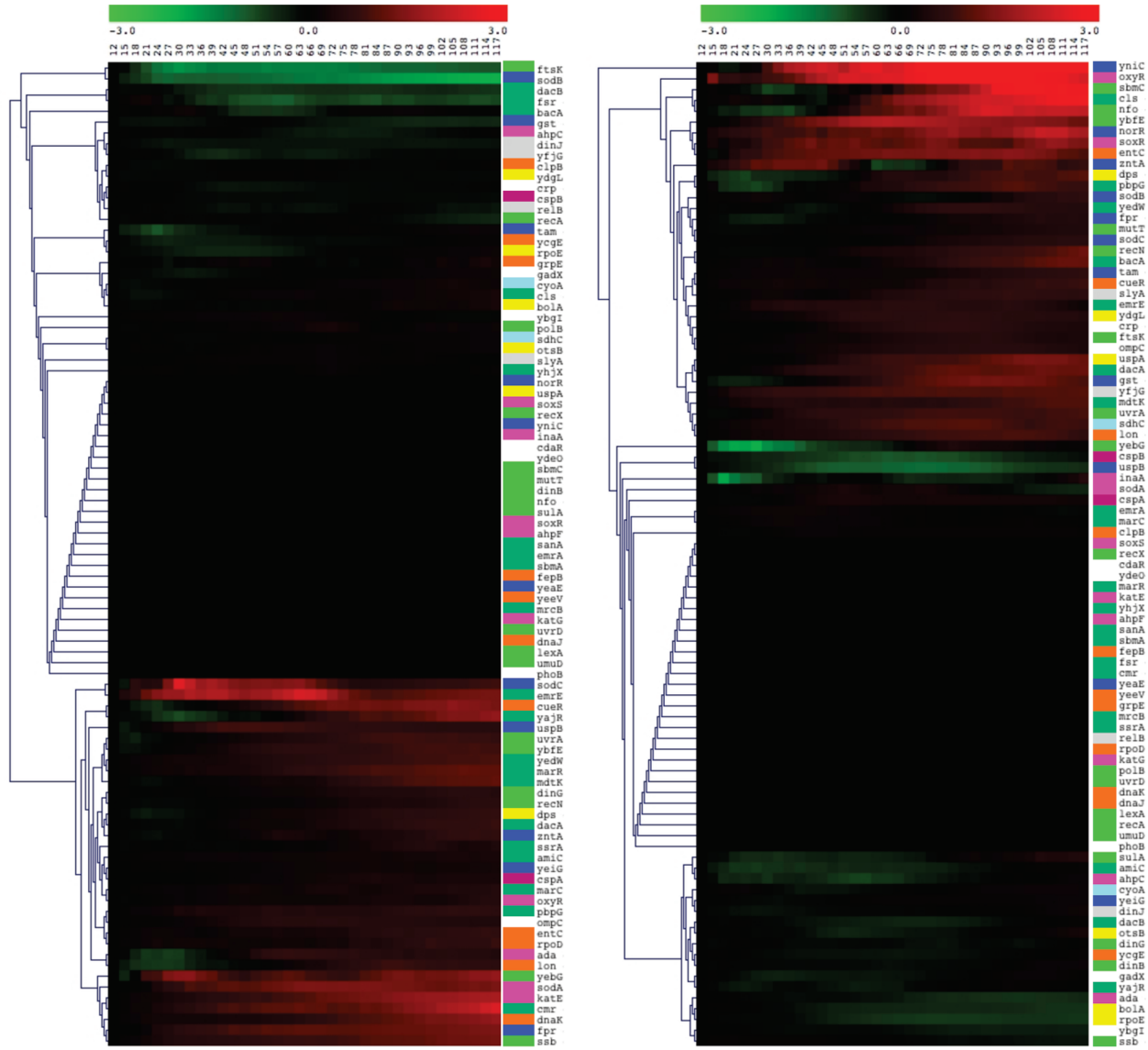

FIGURE 1. Real-time (temporal) gene expression profiles of 91 stress genes in *E. coli* in exposure to nAg 10 mg/L (left) 50 mg/L (right). *X*-axis top: natural log of induction factor (lnI). (Red spectrum colors indicate up-regulation, green spectrum colors indicate down-regulation) and time in minutes (the first data point shown is at 15 min after exposure due to moving average), *Y*-axis left: clustering of the profiles, *Y*-axis-right: list of genes color-coded based on functional categorization (STable 1). Profiles for $nTiO_2$_a are shown in SFigure 1.

Prokaryotic Stress Genes Cell-Library with Transcriptional GFP Fusions. A library of transcriptional fusions of GFP (Open Biosystem, Huntsville, AL) that includes 91 different promoters controlling the expression of genes associated with the most known stress responses and other specific function in *E.coli K12*, MG1655 was employed in this study. Each promoter fusion is expressed from a low-copy plasmid, pUA66 or pUA139, which contains a kanamycin resistance gene and a fast folding *gfpmut2*, that enables the measurement of gene expression at a resolution of minutes with high accuracy and reproducibility (*13*). Each category of stress genes and their main functions are briefly described in our previous study (*12*).

Measuring the Temporal Gene Expression upon Chemical Exposure. Cells were grew in black 96-well plates (Costar, Bethesda, MD) for 2 h at 37 °C until the cultures reached early exponential growth (OD600 about 0.05−0.1), NMs stock solution was added per well to obtain a final concentration of 1, 10, 50 mg/L for nAg and $nTiO_2$_a, respectively. Then the plate was put in a Microplate Reader (SynergyTM HT Multi-Mode, Biotech, Winooski, VT) for simultaneous absorbance (OD600) measurement (cell growth) and fluorescence readings (GFP level, filters 485 nm, 528 nm) at a time interval of 3 min. More detailed description of methods is available in our previous study (*12*).

Data Processing and Analysis. All data were corrected for various controls, including blank with medium control (with and without NMs) and promterless bacterial controls (with and without NMs). The alteration in gene expression, also referred as induction factor I ($I = Pe/Pc$), for a given gene at each time point due to chemical exposure, was represented by the ratio of the normalized gene expression GFP level ($Pe = (GFP/OD)_{experiment}$) in the experiments with NMs exposure to that ($Pc = (GFP/OD)_{control}$) in the control condition without any NMs exposure. Then the natural log of I value (lnI) at every time point was compiled for hierarchical clustering (HCL) analysis that was conducted with MultiExperiment View (MeV) version 4.4. Maximum value of lnI for each gene during the 2 h exposure period was applied for comparison of the differentially expressed genes and a cutoff value of 0.4 ($[\ln(I)]_{abs} = 0.4$, which is corresponding to $I = 1.5$ or $I = 0.67$) was applied based on previous evaluation of the background level noise from various controls as well as the reproducibility assessment with multiple

replicates. Detailed information of data process and clustering analysis are available in our previous study and in the support information (Supporting Information (SI) Appendix S1).

Gene Expression Pathway Analysis. We combined our real-time gene expression data with the known pathway and function of genes on EcoCyc database (http://ecocyc.org/) and the Gene Ontology Database (http://www.geneontology.org/) to obtain insights into the network of the specific genetic pathway upon NMs exposure (*16, 17*).

Determination of No Observed Transcriptional Effect Level (NOTEL). We applied the concept of NOTEL as the maximum concentration of a chemical at which less than 5% of the genes are differentially expressed upon chemical exposure compared to control (*6, 9*). We fit a dose−response curve of the percentage of genes expressed in our "stress library" to the concentrations of chemicals, using a generalized linear model with binomial family. The NOTEL is statistically determined based on the dose-response curve.

Result and Discussion

Distinctive and Complex Real-Time Gene-Expression Profiles for nAg and nTiO$_2$_a. Distinctive temporal gene expression profiles were obtained for nAg and nTiO$_2$_a at three different concentrations and over a 2 h period (Figure 1, SI SFigure 1 and SFigure 2). The results showed very dynamic and complex toxicant-induced real-time gene expressions across the stress genes examined, with most of the genes exhibiting different patterns and varying magnitudes of transcription activities over time. The temporal change in gene expression level reflected the dynamic of the cellular response system and the time sequence for a particular set of gene to be involved, which may depend on the system-level multiple gene activation, signaling pathways and the roles and time-sequence in which they are involved in the stress-response mechanism. (Exemplary temporal gene expression profiles for several genes are show in SI SFigure 3.) These temporal gene expression profiling are compound-specific and concentration-dependent and even the slightest molecular alterations in the cellular system response as result of variation in the concentration of the same toxicant, were captured and reflected (Figure 1 and SI SFigure 1). This validates and highlights the advantage of our approach using real-time gene expression to gain temporal resolution, in contrast to a "snapshot" of the dynamic expression profiles at an selected time point such as microarray.

Concentration-Dependent Expression Profiles. The specific genes and the number of genes differentially expressed upon exposure to the same NM varied with different concentrations. Figure 2A illustrated the number of altered genes that are specific to each concentration as well as the numbers of differentially expressed genes that are common to treatments with different NM concentrations. For both nAg and nTiO$_2$_a, only a few genes showed altered expression compared to control at the lowest concentration (1 mg/L) studied, suggesting the threshold of observable molecular alterations at this concentration. For nAg at 1 mg/L, the three toxin-induced genes are completely different from those induced at higher concentration. Many genes related to general stress, cell killing, cold shock, and energy stress were only differentially expressed at higher nAg concentration of 50 mg/L. For nTiO$_2$_a, four genes showed altered expression at 1 mg/L, including gene *tam* (detoxification) that exhibited overexpression for all three concentrations. Similar conclusions have also been reported following Cu exposure with *Daphnia magna* and arsenic exposure in a human lung cell line (*6, 18*), in which the profile obtained at low concentration was distinct from that obtained at a higher concentration. Vulpe et al. mentioned that the specificity of genes in response to a given toxin decreases as the chemical concentrations increases (*6*). This may be because that at higher concentrations, more genes related to general stress and cell killing become more prevalent as the cell overall integrity becomes compromised and the specific mode of toxicity would be overshadowed by a common global system-stress response.

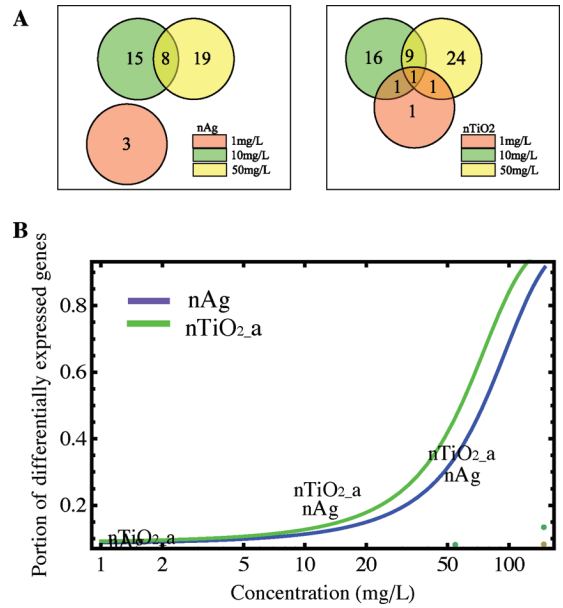

FIGURE 2. Concentration-dependent responses to NMs. (A) Number of differential expressed genes at each exposure concentration. The genes differentially expressed in more than one concentration are shown in the overlapping part, nAg (left), nTiO$_2$ _a (right). (B) Dose−response curve based on the portion of differentially expressed genes upon exposure to NMs in our stress library as a function of NMs concentrations. (Data points are represented by the annotation of NMs.)

The gene expression profiles seem to be not only chemical-specific but also concentration-dependent (Figure 1 and SFigure 1), indicating that the molecular level genomic activities are very sensitive to not only the type of toxicant but also the level of toxicant in exposure. For both nAg and nTiO$_2$_a, the number (percentage) of genes with altered expression level increased as the chemical concentrations increased (Figure 2B). This relationship allowed us to obtain the dose−response curve using a generalized linear model (*6*). For nTiO$_2$_a, concentrations at both 10 mg/L and 50 mg/L induced more genes than nAg, but the induction level are less than those of nAg at the similar concentrations, suggesting lower toxicity level than nAg. This seems to agree with the NMs toxicity level assessment via Biological Oxidative Damage (BOD) proposed by Bello et. al (*15*).

Determination of No Observed Transcriptional Effect Level (NOTEL). The concept of NOTEL was proposed by Lobenhofer et al (*9*) and its potential application in toxicology and risk assessment has been demonstrated and discussed by Ankley and Poynton et al. (*4, 6*). NOTEL can be potentially used as an end point and regulatory benchmark for chemical screening, effluent toxicity testing, and environmental monitoring of toxicant, similar to the end points of traditional toxicity assessment such as EC_{50} and LC_{50}.

The dose−response curve, generated by the number of differentially expressed genes vs the NMs concentration (Figure 2B), allowed for the determination of NOTEL (*6*). In our study, the NOTEL value based on our stress gene library was determined to be 0.658 (±0.260) mg/L for nAg, and 0.557 (±0.545) mg/L for nTiO$_2$_a. The results indicated that these two NMs seemed to have similar magnitude of toxicity, which is consistent with the BOD values for nAg and nTiO$_2$_a recently proposed as 116.4 μmole-TEU (Trolox equivalent units)/L and 64.9 μmole-TEU/L, respectively (*15*). The NOTEL is expected to be lower and more sensitive than conventional

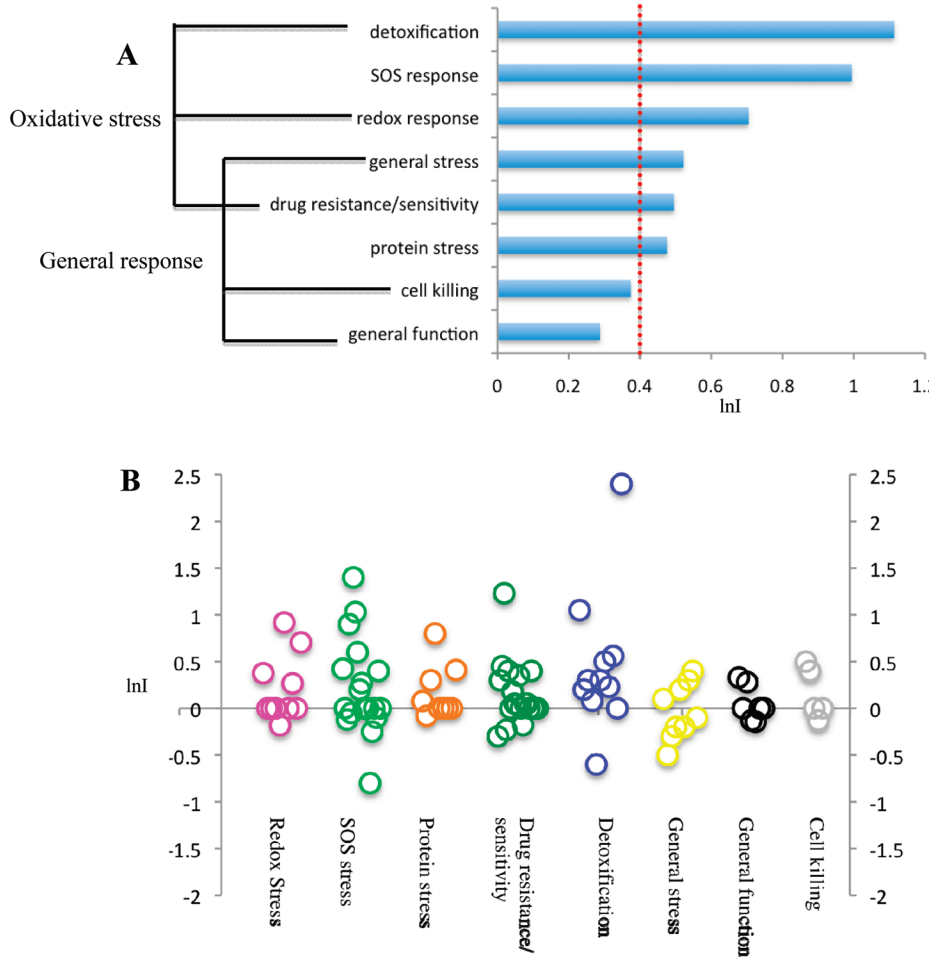

FIGURE 3. Toxicity mechanisms revealed by the altered gene expression level for genes involved in different stress functional categories in exposure to nAg (10 mg/L). (A) Upper limit (at 90% confidence interval) of the average of the maximum altered gene expression level (LnI) for genes involved in each stress functional category. In our study, we chose LnI = 0.4 as the noise cutoff baseline. (B) Distribution of altered gene expression level (LnI) among the genes involved in each stress functional category.

end points (e.g., EC50) since it reflects sublethal and molecular level response to toxicant.

Toxicity Mechanism of nAg. The toxic mechanisms of metal and metal oxidant NMs are still not fully understood and current understanding indicates that the prominent toxic mode of action involves production of reactive oxygen species (ROS), which can damage DNA, RNA and proteins, including a multitude of oxidized base lesions, abasic sites, single and double-strand breaks, all of these can be cytotoxic and mutagenic (*19*). Our results showed that nAg exposure induced many genes that belong to detoxification, SOS response, oxidative/redox stress, drug resistance/sensitivity and protein stress (Figure 3). In addition, many of the genes related with inner membrane and transport system, such as *cmr*, *fsr*, *yajR*, and *emrE*, were up-regulated in exposure to nAg.

Based on our temporal gene expression results and previous pathway framework (*16, 17*), a more detailed network maps for oxidative damage system was developed as shown in Figure 4. They demonstrated the interrelationship among key genes and their temporarily dynamic gene expression in oxide stress regulatory networks upon exposure to nAg. Oxidative damage response system includes genes related to redox response, detoxification and drug resistance. Redox response are regulated by the two redox regulators, namely *oxyR* and *soxR*. Gene *oxyR* was up-regulated at an increasing level over time upon exposure to nAg, indicating the induction of oxidative damage response (Figure 4). OxyR serves as the transcriptional dual regulator to those involved in peroxide metabolism, peroxide protection and redox balance, which involved *sodA*, *sodB*, *sodC*, *katE*, and *katG* (*16*). The protein products of genes *sodA*, *sodB*, and *sodC* are all subunit of superoxide dismutase (*20*), which involve in the degradation of superoxide to hydrogen peroxide, then subsequently hydrogen peroxide transformation into oxygen catalyzed by hydroperoxidase KatG and KatE. The up-regulation of *sodA*, *sodC*, and *katE* in our result indicated superoxide radical and hydrogen peroxide generated upon nAg exposure. SoxR, which is known to control the transcription of the regulator involved in the responses against nitric oxide toxicity (*21*), was found to be up-regulated after 30 min exposure. Activation of *soxR*, induces *soxS* expression, and *soxS*, in turn, activates transcription and participates in controlling several genes involved in oxidative stress, resistance to antibiotics, organic solvents, and heavy metals, such as *nfo*, *inaA*, and *marR* (*16*). The up-regulation of these genes initiated after 60 min and the alteration magnitude increased over time upon exposure to nAg (Figue 4). The expression level of *oxyR* remained increasing for 90 min then declined afterwards (SI SFigure 3), suggesting that at the later stage the over production of OxyR protein functions as a repressor for the gene *oxyR* (*22*).

Genes related to membrane, oxidase complex and electron or ATPase transfer, incuding *bolA*, *cyoA*, and *sdhC*, were also up-regulated upon exposure to nAg (Figure 4). Overexpression of *bolA* induces biofilm formation, and alters the properties of outer membrane (*23*). SdhC is one of two membrane subunits of succinate dehydrogenase, which

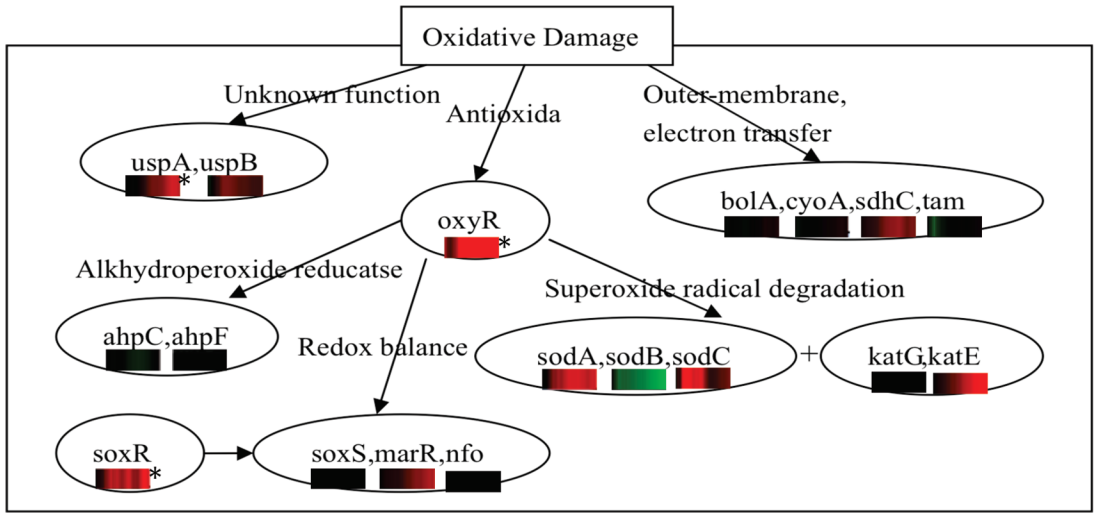

FIGURE 4. Oxidative stress response regulator network upon exposure to nAg based on temporally dynamic gene expressions obtained in our study. Black line with arrow indicates the altered gene expression due to nAg exposure (10 mg/L, except those with "*" are shown at 50 mg/L and they were also altered at 10 mg/L). For each gene, altered expression level upon 2 hours nAg exposure are shown as a colored bar (See color bar scale in Figure 1, red: up-regulated; green: down-regulated; black: neutral).

participates in both the citric acid cycle and the electron transfer chain (*24*). Gene *tam*, which showed up-regulation at the end of 2 h exposure, is a trans-aconitate methyltransferase.

Most drug resistance genes induced by nAg (at 10 mg/L) are major facilitator superfamily (MFS). The MFS transporters are single-polypeptide secondary carriers capable only of transporting small solutes in response to chemiosmotic ion gradients. *cmr*, whose product also known as MdfA, is a multidrug transporter that is driven by the proton electrochemical gradient (*25*) and it showed 3.5 folds overexpression in our results. *emrE*, encoding for a multidrug efflux protein with an broad substrate specificity, exhibited up-regulation by 3 folds. In addition, *fsr*, *yajR*, which were overexpressed at 10 mg/L nAg exposure, belong to the drug efflux systems of MFS. However, none of these genes showed overexpression at 50 mg/L nAg exposure, indicating again that at higher toxin concentration, the entire integrity of bacteria cell is likely compromised such that it lost its specific antitoxin ability. Or, alternatively, bacteria activates overall global-stress response system at a higher concentration, as discussed previously.

Genes involved in DNA repair, such as *recN*, *uvrA*, *ybfE*, *yebG*, *ssb*, *sbmc*, and *nfo*, were up-regulated 30 min after being exposed to nAg. RecN is required for DNA repair when breaks occur at two or more locations. Overexpression of *uvrA*, a subunit of UvrABC nucleotide DNA excision repair complex, indicates its active role in repairing a wide diversity of lesions. The product of the essential *ssb* gene, interacts directly with DNA polymerase II, exonuclease I, and replication protein n, which are all involved in DNA metabolism (*26*). Endonuclease Nfo catalyze the formation of single-stand breaks in double apurinic (AP) DNA to remove the damaged base in DNA repair. Interestingly, the two key upstream regulating genes of SOS system, *recA* and *lexA*, showed no observed differential expression within the two hours period. Previous studies of SOS system generally assume that genes recA and lexA should be up-regulated when SOS system is turned on (*27*, *28*). However, not all SOS genes are regulated by *lexA*, and *recA* are not involved in every physiological DNA repair pathway (*29*). So the involvement and activity of SOS response genes to different genotoxicity may require further investigation. Nevertheless, altered promoter activity of a number of DNA repair related genes discussed above suggested that nAg causes DNA damage.

Toxicity Mechanism of nTiO$_2$_a. The genes differentially expressed upon exposure of nTiO$_2$_a are mostly dominated by those belonging to drug resistance/sensitivity, detoxification, DNA damage and protein stress categories (SI SFigure 2). About one-third of the differential expressed genes induced by nTiO$_2$_a (10 mg/L) are the same as those induced by nAg (10 mg/L), including genes in drug resistance/sensitivity, DNA damage categories, suggesting that both NMs cause oxidative stress and DNA damage. However, the other two-thirds of the altered genes in exposure to nTiO$_2$_a were different for the two NMs. indicating distinctive transcription level stress response these two NMs induce. More than half of the drug resistance/sensitivity genes induced by nTiO$_2$_a (10 mg/L) belongs to MFS, some of them are the same genes with nAg (10 mg/L). However, at concentration of 50 mg/L, less than one-fourth drug resistance/sensitivity genes belong to MFS. Cell membrane transportation related genes including *cmr*, *yajr*, and *emrE*, and *dnaK*, which are involved in the cytoplasmic cellular processes such as protein folding and protein translocation through membranes, were also up-regulated in exposure to nTiO$_2$_a at 10 mg/L. *sanA*, which involves in cell envelope barrier functions, was up-regualted in exposure to nTiO$_2$_a (10 mg/L), indicating outer membrane permeability defects (*30*). These suggested that nTiO$_2$_a damaged the permeability of cell membrane, which was also evidenced by our recent study that observed compromised cell membrane and surface (data not published). AphF, functioned with AphC to catalyze alklhydroperoxide into alcohol with the participation of NAD(P)H, different from the hydroperoxidase KatE (up-regulated in nAg), a key step in superoxide redicals degradation, convert hydrogen peroxide directly into water and oxygen (*31*). As gene *aphF* showed 2 folds overexpression upon nTiO$_2$_a (10 mg/L) but no expression with nAg exposure (10 and 50 mg·L), which may indicate that nTiO$_2$_a induced a different peroxide degradation pathway compared to nAg.

nTiO$_2$_a(10 mg/L) caused DNA damage and it activated the DNA repair SOS system, as indicated by the up-regulations of the two key upstream regulons, *recA* and *lexA*, which showed 1.5-fold and 3-fold overexpression, respectively. Their activation led to the up-regulations of a number of DNA damage related genes, including *recN*, *mutT*, *nfo*, *uvrA*, *uvrD*, *umuD*, *polB*, and *ssb*. DNA polymerase II (Pol II), the product of gene *polB*, is a combined polymerase and exonuclease involved in translesion synthesis and nucleotide excision

repair, and it also plays a role in avoiding the mutagenic effects of agents such as peroxide (*32*).

Candidate Biomarkers for nAg and $nTiO_2$_a Exposure. Compound-specific signature gene expression profile offers the possibility to uncover novel biomarkers of exposure and predict the presence of a class of contaminants (*8, 33*), especially the emerging contaminants such as NMs for which biomarkers are not presently available. Based on the gene expression results, we can propose some genes as potential biomarkers based on the following guidelines (a) genes that show chemical-specific and concentration-dependent expression pattern; (b) genes that are more related to MOA of a contaminant rather than those general stress or function genes. We screened and selected genes that seem to show significant alteration in their expression level and exhibited concentration-dependent patterns as candidate biomarkers for nAg and $nTiO_2$_a exposure. *oxyR*, *cls*, and *cspB* are shown to be the potential biomarkers for nAg exposure and *mutT*, *sodB*, *pbpG* are the three potential biomarkers for $nTiO_2$_a exposure (SI SFigure 3). Of course, the specificity, sensitivity and reliability of these suggested candidate biomarkers require further investigation and evaluation.

In summary, our results, for the first time, revealed more detailed transcriptional information on the toxic mechanism of nAg and $nTiO_2$_a and led to a better understanding of the MOA of metal and metal oxide NMs. Both NMs were found to cause oxidative stress as well as cell membrane and transportation damage. But the difference in the specific genes with altered expression upon the exposure to the two NMs, suggested the different toxic mechanisms. For example, different hydrogen peroxide reduction pathway seemed to be involved in the oxidative stress response, as nAg damage electron transfer pathway, whereas, $nTiO_2$_a damages membrane permeability. Both $nTiO_2$_a and nAg cause DNA damage, however, differences were observed in the genes and their magnitude of alterations involved in the SOS system. In addition, we observed that the NMs at lower concentration tend to induce more chemical-specific toxicity response, while at higher concentrations, more general global response dominates. The information-rich real-time gene expression results allowed for identification of potential biomarkers that can be employed for specific toxin detection and monitoring applications. The NOTEL values determined for both nAg and $nTiO_2$_a seem to be consistent with other established toxicity assessment end points, therefore can be potentially used as regulatory benchmarks and for toxicity screening. Our results demonstrated that real-time gene expression profiling yields compound-specific and concentration-sensitive multidimensional "fingerprints" specific to each compound with variables of gene, time, and concentration and therefore can be applied as a feasible method for toxicity assessment and screening of a large number of emerging contaminants.

Acknowledgments

This study was supported by National Science Foundation (NSF) (EEC-0926284) and National Science Foundation Nanoscale Science and Engineering Center (NSEC) for High-rate Nanomanufacturing (0425826). We thank Prof. Dhimiter Bello and Pal, Anoop K. from University of Massachusetts at Lowell for providing the nanomaterials solutions.

Supporting Information Available

STable 1 provides the list of stress genes included in our whole cell-array and their main functions. SFigure 1 shows the two-dimensional (time and genes) gene expression profiles clustered based on their temporal patterns upon exposure to $nTiO_2$_a (10 and 50 mg/L). SFigure 2 shows the groups of genes based on their temporal pattern of gene expression determined using self-organizing map (SOM). SFigure 3 exhibited the exemplary temporal profiles of representative genes that showed compound-specific and concentration-dependent gene expression profiles. Appendix 1 provides the detailed description of methods for gene expression data processing and analysis applied in our study. This material is available free of charge via the Internet at http://pubs.acs.org.

Literature Cited

(1) Kang, S.; Mauter, M. S.; Elimelech, M. Microbial cytotoxicity of carbon-based nanomaterials: Implications for river water and wastewater effluent. *Environ. Sci. Technol.* **2009**, *43* (7), 2648–2653.

(2) Lanone, S.; Rogerieux, F.; Geys, J.; Dupont, A.; Maillot-Marechal, E.; Boczkowski, J.; Lacroix, G.; Hoet, P. Comparative toxicity of 24 manufactured nanoparticles in human alveolar epithelial and macrophage cell lines. *Part. Fibre Toxicol.* **2009**, *6*, 12.

(3) Snape, J. R.; Maund, S. J.; Pickford, D. B.; Hutchinson, T. H. Ecotoxicogenomics: the challenge of integrating genomics into aquatic and terrestrial ecotoxicology. *Aquat. Toxicol.* **2004**, *67* (2), 143–154.

(4) Ankley, G. T.; Daston, G. P.; Degitz, S. J.; Denslow, N. D.; Hoke, R. A.; Kennedy, S. W.; Miracle, A. L.; Perkins, E. J.; Snape, J.; Tillitt, D. E.; Tyler, C. R.; Versteeg, D. Toxicogenomics in regulatory ecotoxicology. *Environ. Sci. Technol.* **2006**, *40* (13), 4055–4065.

(5) Newton, R. K.; Aardema, M.; Aubrecht, J. The utility of DNA microarrays for characterizing genotoxicity. *Environ. Health Perspect.* **2004**, *112* (4), 420–422.

(6) Poynton, H. C.; Loguinov, A. V.; Varshavsky, J. R.; Chan, S.; Perkins, E. I.; Vulpe, C. D. Gene expression profiling in *Daphnia magna* part 1: Concentration-dependent profiles provide support for the No Observed Transcriptional Effect Level. *Environ. Sci. Technol.* **2008**, *42* (16), 6250–6256.

(7) Watson, W. P.; Mutti, A. Role of biomarkers in monitoring exposures to chemicals: present position, future prospects. *Biomarkers* **2004**, *9* (3), 211–242.

(8) Poynton, H. C.; Zuzow, R.; Loguinov, A. V.; Perkins, E. J.; Vulpe, C. D. Gene expression profiling in *Daphnia magn*a, part II: Validation of a copper specific gene expression signature with effluent from two copper mines in California. *Environ. Sci. Technol.* **2008**, *42* (16), 6257–6263.

(9) Lobenhofer, E. K.; Cui, X. G.; Bennett, L.; Cable, P. L.; Merrick, B. A.; Churchill, G. A.; Afshari, C. A. Exploration of low-dose estrogen effects: Identification of No Observed Transcriptional Effect Level (NOTEL). *Toxicol. Pathol.* **2004**, *32* (4), 482–492.

(10) Williams, T. D.; Diab, A.; Ortega, F.; Sabine, V. S.; Godfrey, R. E.; Falciani, F.; Chipman, J. K.; George, S. G. Transcriptomic responses of European flounder (*Platichthys flesus*) to model toxicants. *Aquat. Toxicol.* **2008**, *90* (2), 83–91.

(11) George, S.; Gubbins, M.; MacIntosh, A.; Reynolds, W.; Sabine, V.; Scott, A.; Thain, J. In *a Comparison of Pollutant Biomarker Responses with Transcriptional Responses in European Flounders (Platicthys flesus) Subjected to Estuarine Pollution*; Elsevier Science Ltd: New York. 2004; pp 571−575.

(12) Onnis-Hayden, A.; Weng, H. F.; He, M.; Hansen, S.; Ilyin, V.; Lewis, K.; Gu, A. Z. Prokaryotic real-time gene expression profiling for toxicity assessment. *Environ. Sci. Technol.* **2009**, *43* (12), 4574–4581.

(13) Zaslaver, A.; Bren, A.; Ronen, M.; Itzkovitz, S.; Kikoin, I.; Shavit, S.; Liebermeister, W.; Surette, M. G.; Alon, U. A comprehensive library of fluorescent transcriptional reporters for Escherichia coli. *Nat. Methods* **2006**, *3* (8), 623–628.

(14) Zaslaver, A.; Kaplan, S.; Bren, A.; Jinich, A.; Mayo, A.; Dekel, E.; Alon, U.; Itzkovitz, S. Invariant distribution of promoter activities in *Escherichia coli*. *PLoS Comput. Biol.* **2009**, *5* (10), 10.

(15) Bello, D. Hsieh, Shu-Feng, Schmidt, Daniel and Rogers, Eugene, Nanomaterials properties vs. biological oxidative damage: Implications for toxicity screening and exposure assessment. *Nanotoxicology* **2009**, *3* (3), 13.

(16) Keseler, I. M.; Bonavides-Martinez, C.; Collado-Vides, J.; Gama-Castro, S.; Gunsalus, R. P.; Johnson, D. A.; Krummenacker, M.; Nolan, L. M.; Paley, S.; Paulsen, I. T.; Peralta-Gil, M.; Santos-Zavaleta, A.; Shearer, A. G.; Karp, P. D. EcoCyc: A comprehensive view of *Escherichia coli* biology. *Nucleic Acids Res.* **2009**, *37*, D464–D470.

(17) Ashburner, M.; Ball, C. A.; Blake, J. A.; Botstein, D.; Butler, H.; Cherry, J. M.; Davis, A. P.; Dolinski, K.; Dwight, S. S.; Eppig, J. T.; Harris, M. A.; Hill, D. P.; Issel-Tarver, L.; Kasarskis,

A.; Lewis, S.; Matese, J. C.; Richardson, J. E.; Ringwald, M.; Rubin, G. M.; Sherlock, G.; Gene Ontology, C. Gene Ontology: tool for the unification of biology. *Nat. Genet.* **2000**, *25* (1), 25–29.
(18) Andrew, A. S.; Warren, A. J.; Barchowsky, A.; Temple, K. A.; Klei, L.; Soucy, N. V.; O'Hara, K. A.; Hamilton, J. W. Genomic and proteomic profiling of responses to toxic metals in human lung cells. *Environ. Health Perspect.* **2003**, *111* (6), 825–838.
(19) Diakowska, D.; Lewandowski, A.; Kopec, W.; Diakowski, W.; Chrzanowska, T. Oxidative DNA damage and total antioxidant status in serum of patients with esophageal squamous cell carcinoma. *Hepato-Gastroenterology* **2007**, *54* (78), 1701−1704.
(20) Alscher, R. G.; Erturk, N.; Heath, L. S. In *Role of Superoxide Dismutases (SODs) in Controlling Oxidative Stress in Plants*; Oxford University Press: New York, 2002; pp 1331−1341.
(21) Tsaneva, I. R.; Weiss, B. SOXR, A locus governing a superoxide response regulon in *Escherichia-coli K-12*. *J. Bacteriol.* **1990**, *172* (8), 4197–4205.
(22) Tao, K.; Makino, K.; Yonei, S.; Nakata, A.; Shinagawa, H. Purification and characterization of the *Escherichia coli* OxyR protein, the positive regulator for a hydrogen peroxide-inducible regulon. *J. Biochem* **1991**, *109* (2), 262–266.
(23) Vieira, H. L. A.; Freire, P.; Arraiano, C. M. Effect of *Escherichia coli* morphogene bolA on biofilms. *Appl. Environ. Microbiol.* **2004**, *70* (9), 5682–5684.
(24) Oyedotun, K. S.; Lemire, B. D. The quaternary structure of the *Saccharomyces cerevisiae* succinate dehydrogenase—Homology modeling, cofactor docking, and molecular dynamics simulation studies. *J. Biol. Chem.* **2004**, *279* (10), 9424–9431.
(25) Edgar, R.; Bibi, E. MdfA, an *Escherichia coli* multidrug resistance protein with an extraordinarily broad spectrum of drug recognition. *J. Bacteriol.* **1997**, *179* (7), 2274–2280.
(26) Meyer, R. R.; Laine, P. S. The single-stranded DNA-binding protein of *Escherichia coli*. *Microbiol. Rev* **1990**, *54* (4), 342–380.
(27) Yamanaka, T.; Toyoshiba, H.; Sone, H.; Parham, F. M.; Portier, C. J. The TAO-Gen algorithm for identifying gene interaction networks with application to SOS repair in *E coli*. *Environ. Health Perspect.* **2004**, *112* (16), 1614–1621.
(28) McCool, J. D.; Long, E.; Petrosino, J. F.; Sandler, H. A.; Rosenberg, S. M.; Sandler, S. J. Measurement of SOS expression in individual *Escherichia coli K-12* cells using fluorescence microscopy. *Mol. Microbiol.* **2004**, *53* (5), 1343–1357.
(29) Walker, G. C. Mutagenesis and inducible responses to deoxyribonucleic acid damage in Escherichia coli. *Microbiol. Rev.* **1984**, *48* (1), 60–93.
(30) Rida, S.; Caillet, J.; Alix, J. H. Amplification of a novel gene, sanA, abolishes a vancomycin-sensitive defect in Escherichia coli. *J. Bacteriol.* **1996**, *178* (1), 94–102.
(31) Bieger, B.; Essen, L. O. Crystallization and preliminary X-ray analysis of the catalytic core of the alkylhydroperoxide reductase component AhpF from *Escherichia coli*. *Acta Crystallogr., Sect. D: Biol. Crystallogr.* **2000**, *56*, 92–94.
(32) Sedliakova, M.; Slezarikova, V.; Masek, F.; Vizvaryova, M.; Pirsel, M. Role of DNA polymerase II in the tolerance of thymine dimers remaining unexcised in UV-irradiated *Escherichia coli* exposed to pre-UV nutritional stress. *J. Photochem. Photobiol., B* **2001**, *65* (2−3), 145–150.
(33) Kim, H. J.; Rakwal, R.; Shibato, J.; Iwahashi, H.; Choi, J. S.; Kim, D. H. Effect of textile wastewaters on *Saccharomyces cerevisiae* using DNA microarray as a tool for genome-wide transcriptomics analysis. *Water Res.* **2006**, *40* (9), 1773–1782.

ES100679F